Earth, Moon, and Planets (2005) 97: 165–175
DOI 10.1007/s11038-006-9067-9
© Springer 2006

Dust Activity in Comet 67P/Churyumov–Gerasimenko from February 20 to April 20, 2003

L. M. LARA and P. J. GUTIÉRREZ
Instituto de Astrofísica de Andalucía, CSIC, P.O. Box 3004, 18080 Granada, Spain
(E-mail: lara, pedroj{@iaa.es})

J. DE LEÓN
Instituto de Astrofísica de Canarias, C/ Vía Láctea s/n, 38200 La Laguna, Tenerife, Spain
(E-mail: jmlc@ot.iac.es)

J. LICANDRO
Isaac Newton Group of Telescopes, P.O. Box 321, 38700 Santa Cruz de La Palma, Tenerife, Spain
(E-mail: licandro@ing.iac.es)

(Received 23 April 2004; Accepted 1 February 2006)

Abstract. Broadband imaging of Comet 67P/Churyumov–Gerasimenko has provided more data on the characterisation of the target of the ESA Rosetta Mission. The comet monitoring between $r_h = 2.37$ and $r_h = 2.78$ AU postperihelion shows a prominent dust coma which extends up to $\approx$ 25,000 km from the nucleus, and a long dust structure in approximately anti-tail direction, reaching at least 230,000 km, identified as a neck-line structure. The non-isotropic dust emission is detected from the structures in the inner coma, and it is reflected on the slope of linear fits of surface brightness profiles vs. cometocentric projected distance in log–log representation as $m \approx 0.83-0.941$. Besides the long dust spike at position angle of 295°, the morphological study of the dust coma confirms the presence of two structures at position angles of ~95 and ~195° where the overabundance of dust can be as high as 50% at $\rho \leq 30{,}000$ km. The $Af\rho$ parameter derived from our R broadband data is 26.0 and 29.8 cm at $r_h = 2.37$ and 2.48 AU postperihelion. The dust reflectivity $S'(\lambda)$, a measurement of the dust colour, is $\sim 0.061 \pm 0.019$, a rather neutral colour.

Keywords: Comets: comet Churyumov–Gerasimenko, Comets: general

1. Introduction

The delay of the Rosetta's launch from January 2003 to February 2004 due to problems with the launch vehicle, meant the identification of alternative mission opportunities. The successful launch on March 2, 2004 established 67P/Churyumov–Gerasimenko (referred ad 67P/C–G in the following) as the target of the Rosetta Mission. Basic properties such as nucleus size, rotation and surface activity, need to be determined (or at least, constrained) to ensure that the rendezvous of the spacecraft with the comet and the subsequent landing of the module *Philae* on the nucleus be successful.

After the discovery of 67P/C–G in 1969, it has been seen only at six apparitions, of which the latest was 2002/2003, with perihelion on August 18, 2002, at $r_h = 1.29$ AU. Since its selection as the new target of the Rosetta Mission, an extensive observation campaign has been carried out from February 2003 until nowadays. Among these observations, Lamy et al. (2003) has shown that the approximate radius of 67P/C–G is about 2 km. Optical observations at $r_h \sim 2.3$ AU postperihelion still show a clear dust coma covering $\approx$ 20,000 km at the comet distance (Schulz, 2003a, 2003b; Weiler et al., 2004), as well as a long neck-line structure due to large dust particles residing in the comet orbital plane likely ejected at $r_h \approx 3$ AU preperihelion (Fulle et al., 2004; Moreno et al., 2004).

We have monitored the comet activity from February 20 to April 20, 2003 from the Observatorio Roque de los Muchachos (La Palma, Spain) and from the Observatorio del Teide (Tenerife, Spain) by taking CCD images with broadband optical filters. Here, an analysis of the dust in comet 67P/C–G is presented: $Af\rho$, structural analysis of the coma, dust colour and intensity (or brightness) as function of projected cometocentric distance ρ.

2. Observations and Basic Data Reduction

Comet 67/Churyumov–Gerasimenko was observed at the Observatorio Roque de los Muchachos (La Palma, Spain), postperihelion on February 20 and March 27, 2003, and at the Observatorio del Teide (Tenerife, Spain) on February 22, March 9, 31, and April 11, 20, 2003. During this period, the comet was moving outbound from $r_h = 2.37$ to $r_h = 2.78$ AU, whereas the geocentric distance increased from 1.42 to 2.04 AU.

Observations at Teide Observatory (Canary Islands, Spain) were done with the 82 cm IAC-80 Telescope. Among the five nights, only February 22 and March 9, 2003 were photometric nights. Charged Coupled Device images were obtained using the Thomson 1024×1024 CCD (pixel size 0″.4325, FOV ~ 7′.3 × 7′.3) and the V and R Johnson filters. For absolute calibration, standard stars (Area 98 on February 22, and Area G45-20 and PG15-228 on March 9, both in Landolt 1992) were observed at different airmasses and in both filters. The observations carried out at La Palma Observatory were done with the camera-spectrograph DOLORES (Device Optimised for the LOw RESolution) mounted at the 3.56 m Telescopio Nazionale Galileo (TNG) and with the U, B, V, and R Johnson filters. In the imaging mode, DOLORES provides a 9′.4 × 9′.4 field of view (0″.275 per pixel plate scale). Neither February 20 nor March 27 was a photometric night being thus impossible to perform a flux calibration. However, images acquired during non-photometric nights can be equally used to analyse the coma morphology, and the intensity profiles vs. cometocentric distance.

TABLE I
Details of the observations.

Date (2003)	Time (UT)	Band	Δ (AU)	r_h (AU)	Scale (km/pixel)	Phase (deg)	PA (deg)	Qual.[d]
February 20	00:20–02:03	U, B, V, R	1.42	2.36	283[a]	9.1	265.1	b
February 22	02:18–03:02	V, R	1.42	2.37	445[b]	8.1	261.1	a
March 9	02:15–03:00	V, R	1.50	2.48	470[b]	4.4	189.5	a
March 27	00:13–01:06	R	1.69	2.62	337[a]	9.8	133.1	c
March 31	21:36–03:32	R	1.74	2.64	546[b]	11.1	129.2	c
April 11[c]	23:53–00:50	V, R	1.89	2.72	593[b]	14.2	122.5	c
April 20[c]	00:50–03:34	B, V, R	2.04	2.78	640[b]	16.3	119.2	c

Δ and r_h are the geocentric and heliocentric distances of the comet during our observations. Phase is the Sun-comet-observer angle. PA refers to the position angle of the extended Sun → target radius vector.
[a] Pixel scale 0.275″ per pixel for TNG–DOLORES.
[b] Pixel scale 0.4325″ per pixel for IAC-80.
[c] Very low S/N, however the dust coma and the thin dust tail is still visible.
[d] Night quality code: a – photometric, b – refracted upper-limb of Moon, c – non-photometric.

Details of the observations are presented in Table I. All of the observations were done while tracking on the comet proper motion.

Reduction of the images has been done as in Lara et al. (2003a) and (2003b). More concisely, the images were reduced by making the overscan correction, and then using very high S/N sky flat-fields obtained each night in order to correct pixel-to-pixel variations to below 1%. After that, all comet images were divided by their exposure times (in seconds) to normalise the image intensities to counts per second. The contribution of the sky was determined by computing the median of the pixels close to the border of the images, since the comet did not fill the field of view, and it was subtracted from each image. Each image was calibrated in flux and the uncertainty in this flux calibration resulted to be 0.015 mag in V and 0.012 in R for February 22, and slightly higher (0.020 and 0.025 in V and R, respectively) on March 9. To obtain the final images of the comet, the position of the comet optocenter in every flux calibrated image was determined by fitting a two-dimensional Gaussian to the innermost 20 pixels of the coma with an uncertainty ≤0.7 pixels. All images were recentered using the derived optocenters and when more than one image was taken with the same filter on each night, they were median combined to increase the S/N.

Examples of the reduced images taken on February 20 and March 31, 2003 at the 82 cm IAC telescope are shown in Figure 1.

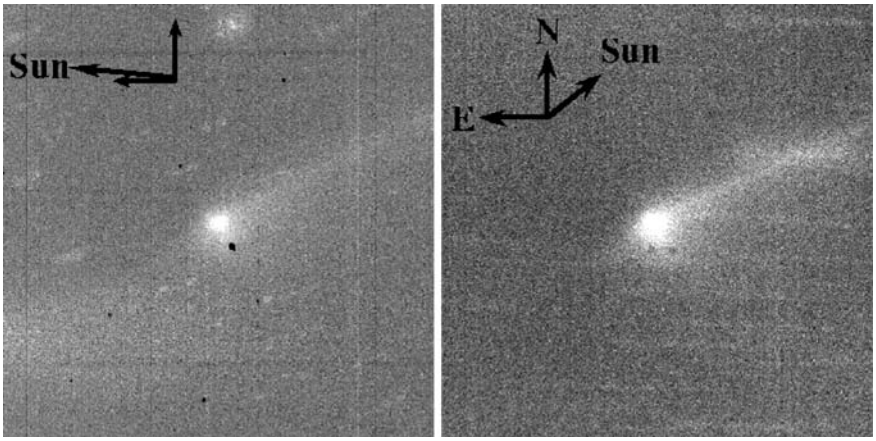

Figure 1. Comet 67P/Churyumov–Gerasimenko as imaged with R Johnson filter on February 22 [left] and March 31 [right], 2003 with the IAC-80cm Telescope. Optocenter (presumed nucleus position) is in the centre of the field of view (FOV) and the display look-up table is linear. The FOV is 346″×346″, meaning 346,000 × 346,000 km and 436,800 × 436,800 km at the comet distance on February 22 and March 31, respectively. Black spot near the dust coma in the left panel is a dead area in the CCD. Both panels have the same orientation, which is only indicated in the right one.

3. Data Analysis and Results

3.1. $Af\rho$, Surface brightness profiles and dust colour

As no clear gas emission (C_2, C_3, NH, NH_2) has been reported at $r_h \sim 2.3$–2.8 AU and only CN (emitting at 3870 Å) has been detected at $r_h = 2.3$ AU with $\log_{10}(Q_{CN}) = (24.2 \pm 3.4) \times 10^{23}$ s^{-1} (Schulz et al., 2004), the gas contamination in broadband V and R images can be considered negligible and therefore, the images mostly contain sunlight scattered by the dust. Thus, an approximate dust production rate can be computed from the flux calibrated frames on February 22 and March 9, 2003. This is done by means of the customary $A\,f\,\rho$ (A'Hearn et al., 1984), and it can be interpreted as the average of the percentage of solar radiation scattered by the cometary dust toward the observer. In terms of measurable quantities, it is equal to

$$Af\rho = \frac{(2\Delta r_h)^2}{\rho}\frac{F_c}{F_S} \tag{1}$$

where Δ and r_h are the comet's geocentric and heliocentric distances, respectively, ρ is the projected radius of aperture, F_c is the measured cometary flux in every filter, and F_S is the solar flux in the same filter.

TABLE II
$Af\rho$ and slopes of the linear fits to the the continuum profiles, in log–log representation, from February 20 to March 31, 2003.

Date (2003)	r_h (AU)	$Af\rho$[a] [cm]		m[b]	
	AU	V	R	V	R
February 20	2.36				
February 22	2.37	25.1	26.0	0.96	0.94
March 9	2.48	28.2	29.8	0.98	0.91
March 27	2.62				0.84
March 31	2.64				0.83

[a] Uncertainties on $Af\rho$ as propagated from reduction and flux calibration are ≤ 5%.
[b] Linear fit for the region $3.2 \leq \log \rho \leq 4.6$ (i.e. $1600 \leq \rho \leq 40{,}000$ km). Standard deviation of the fits ≤3% for February 22 and March 09, whereas it is slightly higher (~ 9%) for the other dates.

This parameter has been derived for the two only photometric nights (February 22 and March 9, 2003) the comet was observed in R broadband filter. The resulting $Af\rho$ values for a circular aperture of 25,000 km at the comet distance are listed in Table II. The obtained values are in line with those previously presented by Storrs et al. (1992), Osip et al. (1992), Kidger (2003), Schulz (2003b) and Schulz et al. (2004). For the time of our observations, $Af\rho$ ranges from 26.0 to 29.8 cm between $r_h = 2.37$ and 2.48 AU postperihelion. Figure 2 shows a comparison of the value deduced in this work and those obtained from other observations of 67P/C–G from February 11 to May 5, 2003, that is, after the 2002 perihelion.

To obtain brightness dust profiles, we azimuthally averaged all of the available median combined images. However, images acquired on February 20 are contaminated by refracted upper-limb of the Moon, whereas those acquired on April 11 and 20 have very low S/N, however the dust coma and the neck-line are still visible. Thus, the behaviour of the brightness profiles vs. projected cometocentric distances has been only studied for February 22, March 9, 27 and 31. Note that this behaviour does not depend on flux calibration and the derived slopes for non-photometric observations are equally meaningful.

Figure 3 shows two examples of the brightness profiles vs. ρ derived from an azimuthal average of the R broadband images in a log–log representation and the corresponding linear fits for $3.2 < \log \rho < 4.6$, i.e. between 1.6×10^3 and 4.0×10^4 km projected radial distance from the nucleus. The values of the slopes of the fits in Figure 3 together with those for March 27 and 31, are listed in Table II, m being comprised between 0.83 and 0.94. The expected dependency according to ρ^{-m} (with $m \approx 1$) in the case of a steady and

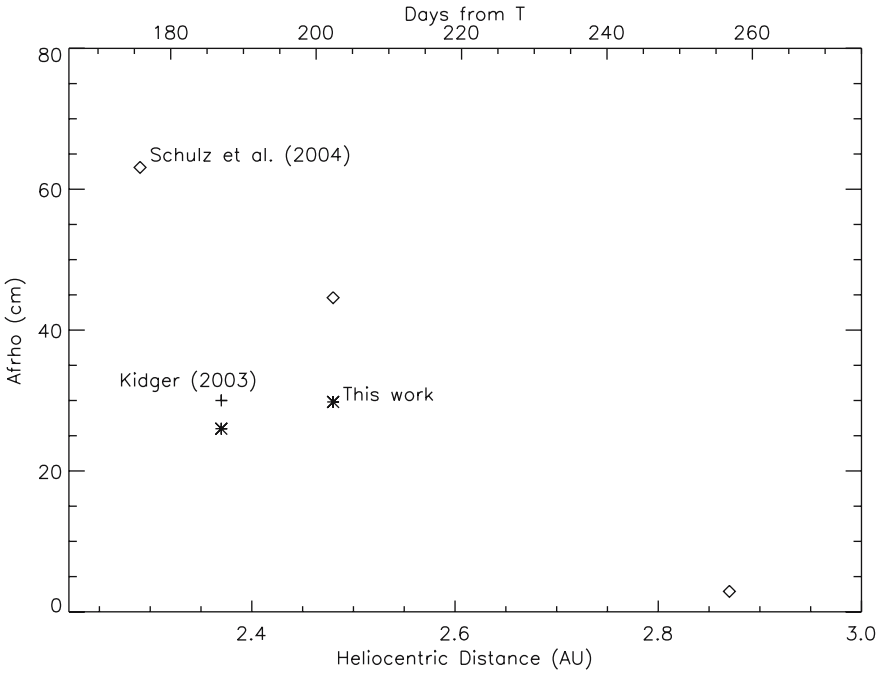

Figure 2. $Af\rho$ (in cm) from February 11 to May 5, 2003. Values provided by Kidger (2003) from amateur astronomers are represented by a single point at T + 188 days (that is, February 22, 2003) for an easy comparison with the results presented here.

isotropic emission of long-lived grains is relatively well fulfilled on every date taking into account the uncertainties in the data reduction, flux calibration and standard deviation of the log–log linear fits.

Colour is measured using the reflectivity $S(\lambda)$, the ratio of the comet intensity with the solar intensity at the same wavelength interval. The nor-

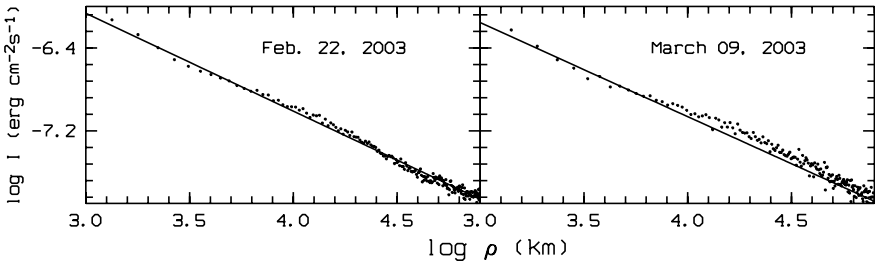

Figure 3. Observed and best linear fits of the dust brightness profiles of comet 67P/C–G in log–log representation for flux calibrated images acquired in R Johnson on February 20 and March 9, 2003. The slopes and standard deviation of these fits are listed in Table II. Error bars in the slopes are ≤ 14% derived from the data reduction, flux calibration and standard deviation of the fit.

malized colour, $S'(\lambda)$, measured as %/100 nm, is often referred as the dust colour or reddening. It can be computed from the $A\,f\,\rho$ parameters listed in Table II as

$$S'(\lambda) = \frac{200}{(Af\rho_1 + Af\rho_2)} \frac{(Af\rho_1 - Af\rho_2)}{(\lambda_1 - \lambda_2)} \tag{2}$$

where 1 and 2 refer to the long and short wavelength. On February 22 and March 9, 2003 the comet was imaged with R and V Johnson filter at the IAC80, being the central wavelength 600 and 525.5 nm, respectively. Hence, from the values of $A\,f\,\rho$ in Table II, an average dust colour $S'(\lambda)$ of 0.047%/100 nm and 0.074%/100 nm is obtained for those two dates, respectively. A rather neutral colour has been also reported by Weiler et al. (2004) from data acquired during the 1996 perihelion passage.

The two dimensional dust colour maps have been also computed from the images acquired on February 22 and March 9, 2003. None of these maps show clear colour variations as a function of ρ.

3.2. 2D Morphology

In every broadband filter and on every date, at first the comet only shows a slightly asymmetric dust coma and a bright thin dust structure at ~ 295°, as measured from north toward east, which extends at least up to 230,000 km from the nucleus. To enhance the existing structures we have applied a Laplace filter (Richter, 1991; Richter et al., 1991; Boehnhardt and Birkle, 1994) to those images where the S/N is high enough to detect features as jets, spikes, fans, etc. This has been only possible on the images acquired on March 27, 2003, as presented in Figure 4.

A further analysis was also carried out on the March 27 image by means of the radial renormalization technique, which enhances deviations from azimuthal symmetry within the coma. An average of the so obtained azimuthal profiles between several cometocentric radial distances provides a clear vision of the structures in the dust coma as displayed in Figure 5.

At ~295°, the neck-line structure is clearly visible when averaging the azimuthal profile at large cometocentric distances (dashed line in Figure 5). Beside this large structure, the dust coma of 67P/C–G also shows two jet-like features at position angles ~ 95 and ~ 195° (as measured from north toward east) detected at close cometocentric distances. These structures have been also identified by Weiler et al. (2004) and named ''B'' and ''A'', respectively. Let us note that the broad feature at ~ 95° (solid line in Figure 5) might partially arise from a background star or galaxy that cannot be completely removed, thus the angular position of the real dust coma structure can be

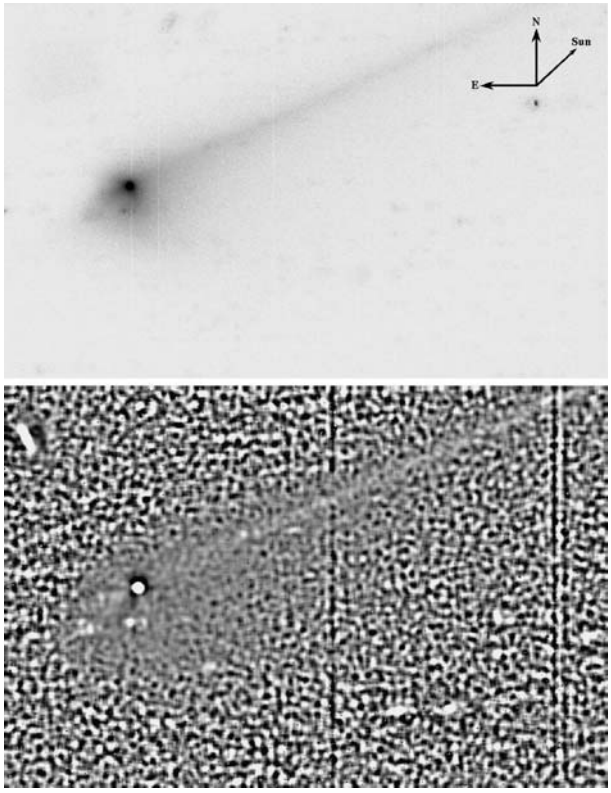

Figure 4. Broadband R image of Comet 67P/Churyumov–Gerasimenko acquired with the 3.56 m TNG on March 27, 2003, after bias and flat-field correction (top), and processed with a Laplacian filter (bottom). North is up and East to the left. The field of view is 247″ × 165″, that is 491,400 × 327,600 km at the comet distance. The dust coma extends up to ρ ~25,000 km, whereas the spike reaches at least $\rho \sim 230{,}000$ km (note that the comet was clipped at the north edge of the CCD). In the raw image, beside the neck-line structure, two other structures approximately in anti-Sun direction (~130°) and at ~195° are seen. The processed image clearly shows the dust spike, whereas the other two structures are not undoubtedly detected. Some artefacts due to bad columns, background stars and a galaxy (upper-left corner) can be seen.

inaccurate by several degrees. Moreover, from the average of the azimuthal profile at large cometocentric distance (i.e. between 66,000 and 80,000 km, dash-dotted line in Figure 5), an increase of intensity at ~ 115° can be seen. This structure undoubtedly corresponds with the 180° extension of the neck-line structure claimed by Weiler et al. (2004). Although the comet was monitored from February 20 to April 20, 2003 and it is likely that the coma structures did exist for the 2 months, only the images acquired on March 27, 2003 have a significantly high S/N to perform such a morphological analysis. This hampers our effort of determining some rotational parameters from the follow-up of the structures as projected on the plane of the sky.

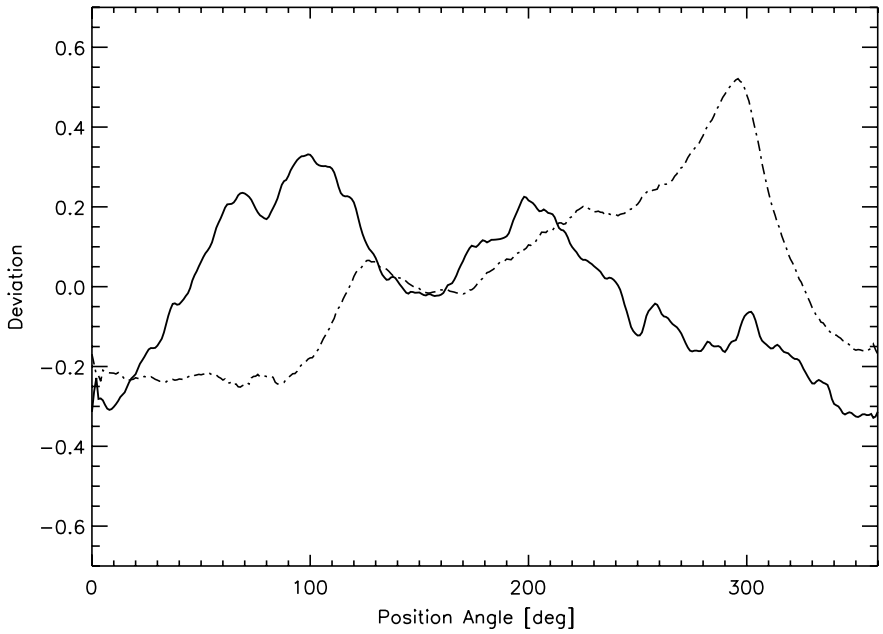

Figure 5. Deviation of the mean coma intensity profile for observations on March 27, 2003 at different cometocentric distances as a function of the azimuthal angle. The profiles have been obtained by averaging the emission between (i) 10,000 and 23,000 km – solid line, and (ii) 66,000 and 80,000 km – dash-dotted line, projected nucleocentric distance. For the inner coma, two features are clearly detected at position angles ~95° (partly arising from a background star or galaxy) and at ~195°. At larger cometocentric distances, a clearly defined structure at 295° is identified which corresponds to the widely reported neck-line, and another one at 180° from this one, that is, at 115°. Secondary peaks at some position angles (specially the one at ~65°) are due to non-perfect removal of background stars.

We have also tried to quantify the enhancement of dust column density as a function of the projected cometocentric distance, ρ at those angular positions (e.g. 95, 195 and 295°) where structures are located. The brightness radial profiles – normalised to the isotropic component – at azimuthal angles of 95, 195 and 295° are shown in Figure 6. At the position angle of the neck-line (~295°), the overabundance of dust increases as much as a factor of 2 with respect to the mean radial profile beyond 40,000 km, mostly because the dust coma does not considerably extend beyond ~25,000 km. In the inner coma, the dust column density at 295° is not significantly below the averaged value in the whole coma.

At ~95° the dust column density is ~20% higher than at other azimuthal positions at cometocentric distances shorter than 20,000 km. In the case of the structure at 195°, the enhancement of the dust column density as a function of ρ results from the overlapping of the 180° extension of the neck-line in the outer coma with the structure at ~95° (see Figure 5) not being

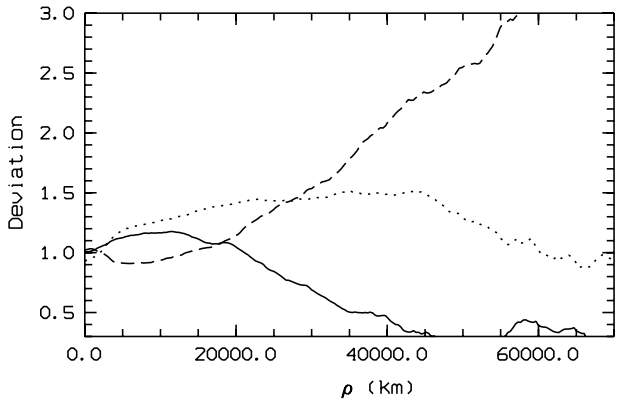

Figure 6. Quotient of the dust radial profiles at selected angles and the azimuthally averaged radial profile. The selected angular positions are those where structures are detected in the coma. Solid line: 95°, dotted line: 195° and dashed line: 295°.

possible to discern up to which distance each structure is dominating the morphology of the coma. The latter can be better seen in Figure 5, where azimuthal profiles averaged in the region 10,000–23,000 km and 66,000–80,000 km are undoubtedly different.

4. Summary

The presence and evolution of the bright thin tail in the dust environment of the Comet 67P/C–G has been reported during 9 months after August 2002 perihelion.

Dust brightness profiles vs. ρ in log–log representation are relatively well fit with $m \approx 1$, within error bars, the slopes being between 0.83 and 0.94. Regardless this quasi-isotropy of the dust coma, enhancement techniques applied to the images show that there are four prominent structures: two jet-like structures at position angles ~95 and ~195°, the neck-line at ~295°, and a fainter one at ~115° considered as the neck-line extension in approximately anti-Sun direction. Within these structures, the radial profiles exhibit different slopes from the mean radial profiles, as well as an increased (up to 40%) or slightly depleted dust column density vs. ρ compared to the overall dust coma.

At heliocentric distances ranging from 2.37 to 2.48 AU, the deduced $A f\rho$ parameter varies from 26.0 to 29.8 cm, respectively. The 67P/C–G dust coma has a rather neutral colour $S'(\lambda) \approx 0.055 \pm 0.02$, independent of the position angle and ρ. This neutral dust colour has been also reported by Weiler et al. (2004) from observations during the 1996 perihelion passage.

Acknowledgements

This work was based on observations made with the 0.80 m IAC80 Telescope at Observatorio del Teide of the Instituto de Astrofisica de Canarias (Tenerife, Spain), and with the Italian Telescopio Nazionale Galileo (TNG) operated on the island of La Palma by the Centro Galileo Galilei of the INAF (Istituto Nazionale di Astrofisica) at the Spanish Observatorio del Roque de los Muchachos of the Instituto de Astrofísica de Canarias. We also thank E. Oliva for kindly providing us with the observations of 67P/C–G taken on March 27, 2003 during DDT. The research carried out has been partially supported by the Spanish Ministerio de Ciencia y Tecnología under contract ESP2003-00357. P. J. Gutiérrez acknowledges the European Space Agency for an External Research Fellowship at LAM.

References

A'Hearn, M. F., Schleicher, D. G. and Feldman, P. D. et al.: 1984, *Astron. J.* **89**, 579–591.
Boehnhardt, H. and Birkle, K.: 1994, *Astron. Astrophys.* **107**, 101–120.
Fulle, M., Barbieri, C., Cremonese, G., Rauer, H., Weiler, M., Milani, A. and Ligustri, R.: 2004, *Astron. Astrophys.* **422**, 357–368.
Kidger, M. R.: 2003, *Astron. Astrophys.* **408**, 767–774.
Lamy, P. L., Toth, I., Weaver, H., Jorda, L. and Kaasalainen, M.: AAS, DPS 35, 30.04, 2003.
Lara, L. M., Licandro, J., Oscoz, A. and Motta, V.: 2003a, *Astron. Astrophys.* **399**, 763–772.
Lara, L. M., Licandro, J. and Tozzi, G. P.: 2003b, *Astron. Astrophys.* **404**, 373–378.
Moreno, F., Lara, L. M., Muñoz, O. and Molina, A.: 2004, *Astrophys. J.* **613**, 1263–1269.
Osip, D., Schleicher, D. G. and Millis, R. L.: 1992, *Icarus* **98**, 115–124.
Richter, G. M.: 1991, *Proceedings of the 3rd ESO Workshop on Data Analysis*, 37.
Richter, G. M., Lorenz, H., Bohm, P. and Priebe, A.: 1991, *Astron. Nachr.* **312**, 345–349.
Schulz, R.: 2003a, in "ROSETTA Science Working Team Meeting", April 2–3, 2003.
Schulz, R.: 2003b, in Abstract book of "The New Rosetta Targets Meeting", p. 10.
Schulz, R., Stuewe, J. and Boehnhardt, H.: 2004, *Astron. Astrophys.* **422**, L19–L21.
Storrs, A. D., Cochran, A. L. and Barker, E. S: 1992, *Icarus* **98**, 163–178.
Weiler, M., Rauer, H. and Helbert, J.: 2004, *Astron. Astrophys.* **414**, 749–755.